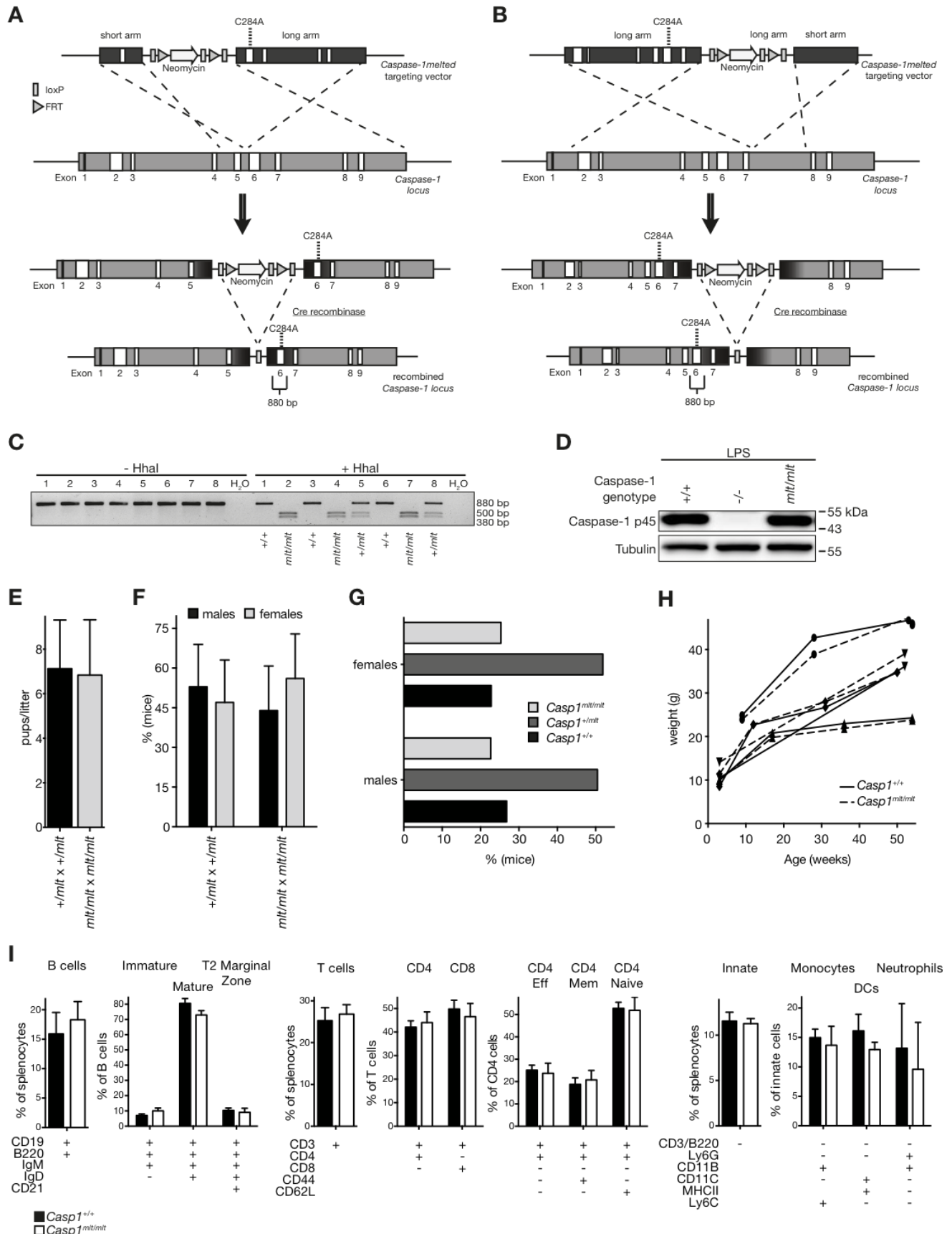


**Cell Reports, Volume 21**

**Supplemental Information**

**The Inflammasome Drives GSDMD-Independent  
Secondary Pyroptosis and IL-1 Release  
in the Absence of Caspase-1 Protease Activity**

**Katharina S. Schneider, Christina J. Groß, Roland F. Dreier, Benedikt S. Saller, Ritu Mishra, Oliver Gorka, Rosalie Heilig, Etienne Meunier, Mathias S. Dick, Tamara Ćiković, Jan Sodenkamp, Guillaume Médard, Ronald Naumann, Jürgen Ruland, Bernhard Kuster, Petr Broz, and Olaf Groß**



**Figure S1. Supplemental data corresponding to main Figure 1: Generation and characterization of *Casp1<sup>mit</sup>* mice**

(A, B) Schematics of the *Casp1<sup>mit</sup>* targeting strategies used in 129 (A) and C57BL/6 (B) stem cells. The region amplified by the genotyping PCR is indicated.

(C) Exemplary genotyping for the *Casp1<sup>mit</sup>* mutation by PCR. The restriction enzyme *HhaI* cuts the mutated site in the amplicon and results in two cleavage product bands in gel electrophoresis.

(D) Immunoblot analysis of caspase-1 protein expression in BMDCs from wild-type, B6.129-*Casp1<sup>-/-</sup>* and B6.129-*Casp1<sup>mit/mit</sup>* mice after LPS priming.

(E) Litter sizes of B6.129-*Casp1<sup>+/mit</sup>* x B6.129-*Casp1<sup>+/mit</sup>* breeding pairs were compared to B6.129-*Casp1<sup>mit/mit</sup>* x B6.129-*Casp1<sup>mit/mit</sup>*.

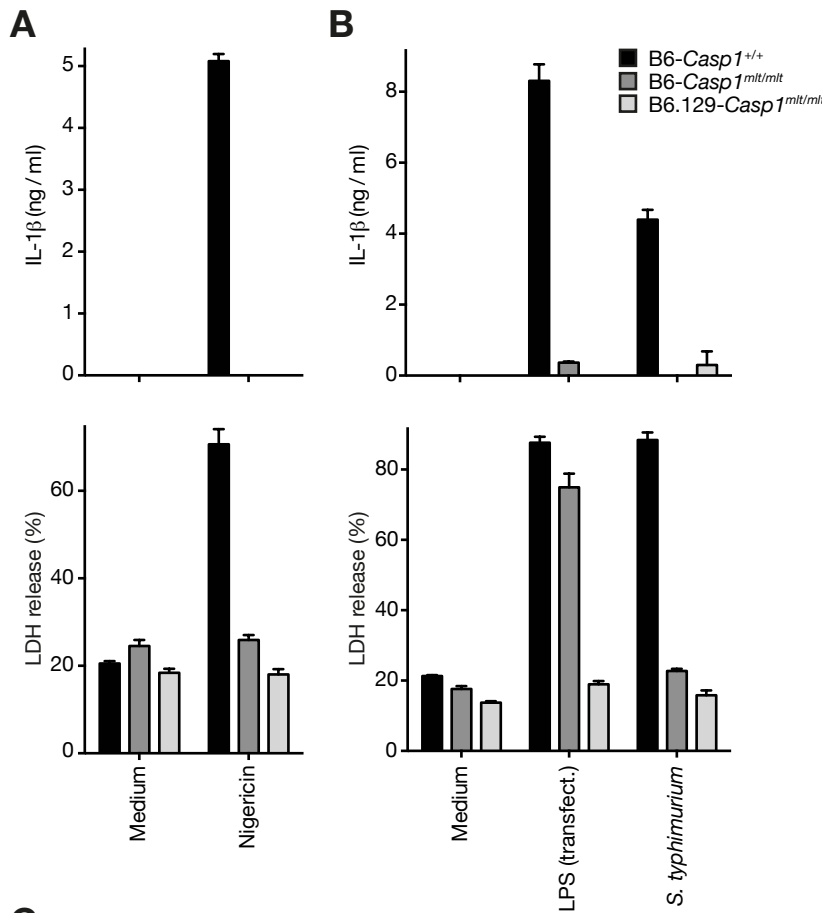
(F) Percentage of male and female pups born from heterozygous (B6.129-*Casp1<sup>+/mit</sup>* x B6.129-*Casp1<sup>+/mit</sup>*) or homozygous (B6.129-*Casp1<sup>mit/mit</sup>* x B6.129-*Casp1<sup>mit/mit</sup>*) *Casp1<sup>mit</sup>* breeding pairs.

(E and F) Heterozygous breeding pairs: n= 23, pups n= 183; homozygous breeding pairs: n= 8, pups n=69.

(G) Analysis of the distribution of *Casp1* genotypes in male and female pups born from heterozygous B6.129-*Casp1<sup>mit</sup>* breeding pairs (male pups n= 100; female pups n= 83).

(H) Weight development of four littermate pairs of one wild-type and one B6.129-*Casp1<sup>mit/mit</sup>* mouse each was monitored over  $\geq 50$  weeks.

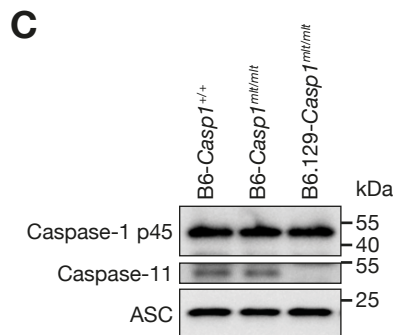
(I) Representative data from FACS analysis of various immune cell compartments from the spleens of wild-type and B6.129-*Casp1<sup>mit/mit</sup>* mice (n= 4 mice per group). Cells were phenotypically defined as indicated and are depicted as mean  $\pm$  s.d. of the indicated population.



**Figure S2. Supplemental data corresponding to main Figure 1: Non-canonical caspase-11 inflammasome activation in B6-Casp1<sup>mt</sup> cells**

(A, B) BMDCs derived from B6-Casp1<sup>+/+</sup>, B6-Casp1<sup>mt/mt</sup>, and B6.129-Casp1<sup>mt/mt</sup> mice were primed with 50 ng/ml LPS (A) or 1 μg/ml Pam3CSK4 (B) for 3h and subsequently stimulated with 5 μM nigericin for 45 min (A), transfected with 10 μg/ml LPS for 16h, or infected with *S. typhimurium* (MOI 20) for 2h (B). Secretion of IL-1β and release of LDH into the supernatant were measured by ELISA and with a colorimetric assay, respectively (mean ± s.e.m. are shown).

(C) BMDCs of the different genotypes as in A, B were analyzed by immunoblotting for the presence of caspase-1 and caspase-11.



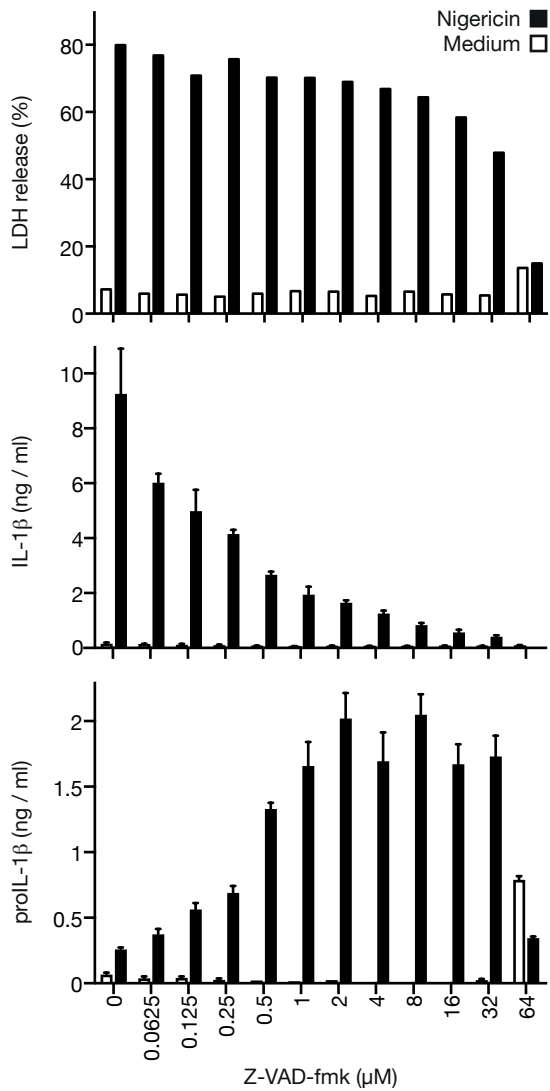


**Figure S3. Supplemental data corresponding to main Figure 3: Effect of Z-VAD-fmk on IL-1 $\beta$  secretion and cell viability**

Supernatants of wild-type BMDCs primed with 50 ng/ml LPS for 3h and stimulated with 5  $\mu$ M nigericin for 45 min were analyzed for secretion of proIL-1 $\beta$  and IL-1 $\beta$  by ELISA and release of LDH by an enzymatic assay in the presence of the indicated doses of the pan-caspase inhibitor Z-VAD-fmk (mean  $\pm$  s.e.m. are shown, data representative of two independent experiments).

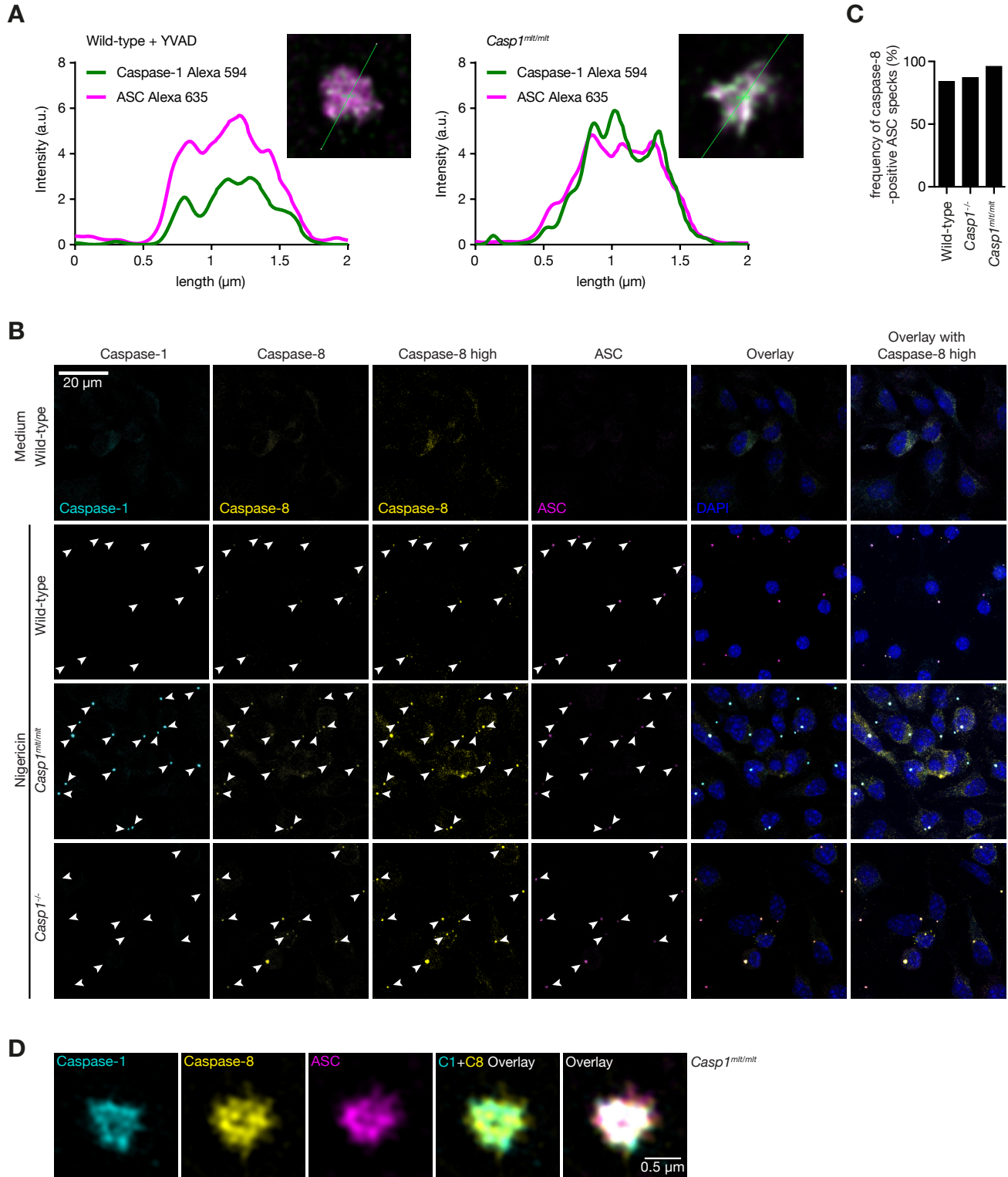


**Figure S4. Supplemental data corresponding to main Figure 4 and 5: Caspase-1<sup>mit</sup> and Caspase-8 accumulate at the inflammasome**

(A) Line intensity profiles of a region of interest of ASC specks from nigericin-stimulated wild-type + Ac-YVAD-cmk (left) or B6.129-Casp1<sup>mit/mit</sup> (right) BMDCs imaged by high resolution STED microscopy as in main Figure 4B. The graphs represent the intensities of caspase-1 (green) or ASC (magenta) at the line drawn in the speck.

(B) LPS-primed BMDCs from B6.129-Casp1<sup>mit/mit</sup> and -Casp1<sup>-/-</sup> mice on culture slides were stimulated with 10  $\mu$ M nigericin for 45 min or left unstimulated (medium) as in main Figure 5A. Cells were then fixed, immunofluorescence stained for caspase-1 (cyan), caspase-8 (yellow), and ASC (magenta), and confocal imaging was performed. DAPI (blue) localizes with the nuclei. Scale bar represents 20  $\mu$ m (data representative of >5 independent experiments). Caspase-8 images are depicted in two different signal intensities to allow evaluation of the frequency of caspase-8 recruitment to the ASC speck. ASC specks are indicated by arrows.

(C) Frequency of caspase-8 colocalization with ASC specks was determined in >100 specks from images obtained in four independent experiments.

(D) A slice through the middle of 3D projection of an ASC speck by SIM imaging depicting the arrangement of caspase-1 (cyan), caspase-8 (yellow) and ASC (magenta). LPS-primed BMDCs of B6.129-Casp1<sup>mit/mit</sup> mice on culture slides were stimulated with 10  $\mu$ M nigericin for 45 min, fixed, and immunofluorescence staining was performed. ASC speck was visualized at high resolution by 3D SIM imaging and z-sections were reconstructed as 3D projections.

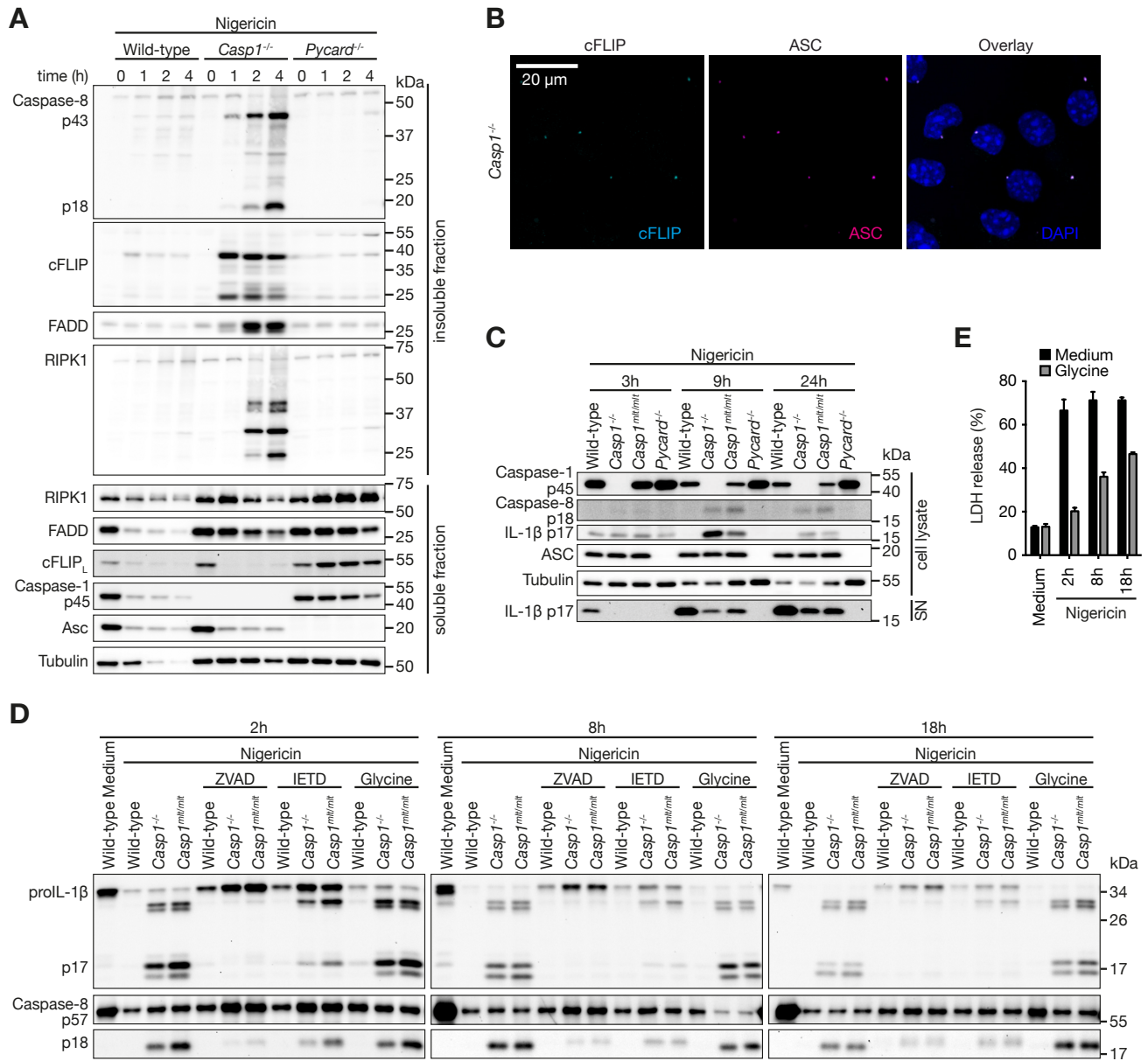


**Figure S5. Supplemental data corresponding to main Figure 5 and 6: Enhanced activation of caspase-8 in cells expressing caspase-1<sup>mit</sup>**

(A) BMDCs of wild-type, B6.129-Casp1<sup>-/-</sup>, and Pycard<sup>-/-</sup> mice were LPS-primed (50 ng/ml) for 3h and subsequently stimulated with 5 μM nigericin for up to 4h. NP-40-insoluble fractions of the cells were isolated by centrifugation and insoluble and soluble fractions analyzed by immunoblotting for presence and processing of caspase-8, cFLIP, FADD, RIPK1, caspase-1, and ASC.

(B) LPS-primed B6.129-Casp1<sup>-/-</sup> BMDCs on culture slides were stimulated with 10 μM nigericin for 45 min, fixed, and then immunofluorescence stained for cFLIP (cyan) and ASC (magenta), and confocal imaging was performed. DAPI (blue) localizes with the nuclei. Scale bar represents 20 μm.

(C) Immunoblot analysis of caspase-8, caspase-1, and IL-1 $\beta$  maturation and secretion up to 24h after inflammasome activation by 5  $\mu$ M nigericin in LPS-primed (50 ng/ml) BMDCs of inflammasome-competent vs. -incompetent mice as indicated (SN= supernatant; data representative of two independent experiments; B6-*Casp1<sup>mt/mt</sup>*).

(D) Immunoblot analysis of caspase-8 and pro-IL-1 $\beta$  maturation after inflammasome activation by 5  $\mu$ M nigericin in LPS-primed (50 ng/ml) B6-caspase-1 mutant BMDCs as indicated in the presence or absence of caspase inhibitors Z-VAD-fmk (20  $\mu$ M), IETD-fmk (20  $\mu$ M), or glycine (500  $\mu$ M; data representative of three independent experiments).

(E) LPS-primed wild-type BMDCs mice were pretreated with 500  $\mu$ M glycine and stimulated with nigericin (5  $\mu$ M) for 2, 8, and 18h. Release of LDH into the supernatant was assessed by an enzymatic assay.

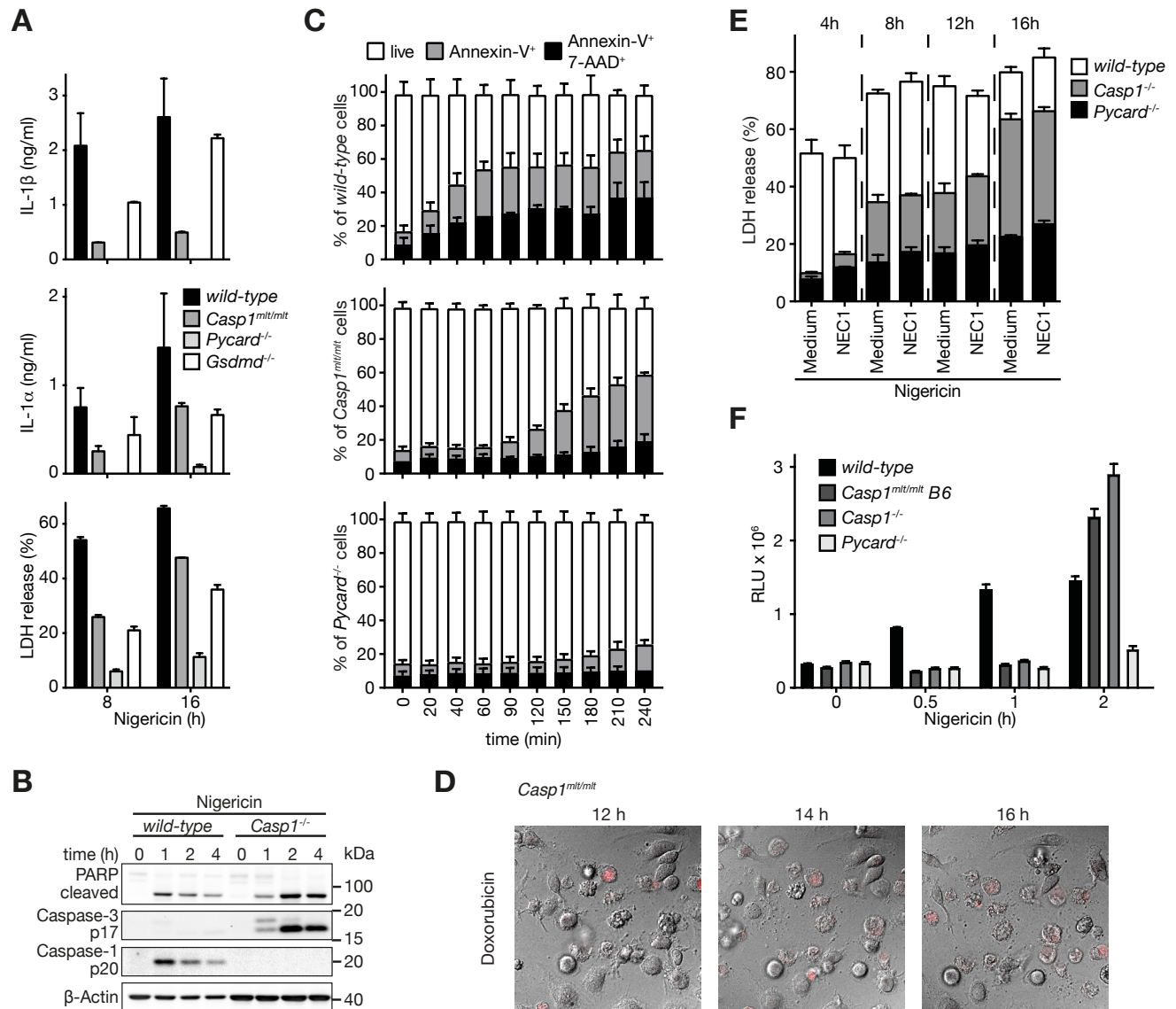


**Figure S6. Supplemental data corresponding to main Figure 6: GSDMD-dependent pyroptosis suppresses caspase-8 activation**

(A) BMDCs of wild-type, B6.129-*Casp1<sup>mlt/mlt</sup>*, *GSDMD<sup>-/-</sup>*, and *Pycard<sup>-/-</sup>* mice were LPS-primed and stimulated with nigericin (5  $\mu$ M) for 8 and 16h. Release of IL-1 $\beta$ , IL-1 $\alpha$ , and LDH into the supernatant were assessed by ELISA and an enzymatic assay, respectively.

(B) BMDCs from wild-type and B6.129-*Casp1<sup>-/-</sup>* mice were LPS-primed (50 ng/ml) for 3h and subsequently stimulated with 5  $\mu$ M nigericin for up to 4h and analyzed by immunoblotting for presence of the processed form of PARP, caspase-3, and caspase-1.

(C) Viability of LPS-primed BMDCs of wild-type, B6-*Casp1<sup>mlt/mlt</sup>*, and *Pycard<sup>-/-</sup>* mice stimulated with nigericin (5  $\mu$ M) for the indicated time-points. Cells were harvested simultaneously and stained for Annexin-V and 7-AAD before analysis by flow cytometry. The bar graphs show the stacked percentages of live (Annexin-V<sup>neg</sup> 7-AAD<sup>neg</sup>), Annexin-V<sup>+</sup>, and Annexin-V<sup>+</sup> 7-AAD<sup>+</sup> cells for the given genotypes (mean  $\pm$  s.d. of three independent experiments).

(D) LPS-primed BMDCs from B6.129-*Casp1<sup>mtl/mtl</sup>* mice on glass chambered coverslips as in Figure 6D were stimulated with doxorubicin and monitored for morphological changes for up to 16h by DIC and fluorescence microscopy. DRAQ7 (red) stains DNA upon loss of membrane integrity.

(E) Lytic cell death over time as indicated was compared by means of LDH release from BMDCs of wild-type, B6.129-*Casp1<sup>-/-</sup>*, and *Pycard<sup>-/-</sup>* mice, which were LPS-primed and nigericin-stimulated in the presence or absence of the necroptosis inhibitor Nec-1.

(F) LPS-primed BMDCs of the indicated genotypes were activated with nigericin (5  $\mu$ M); cleavage of a synthetic caspase-1 substrate was assessed by luminescent emission 0, 0.5, 1, and 2h after stimulation.

## SUPPLEMENTAL EXPERIMENTAL PROCEDURES

### Generation of *Casp1<sup>mit</sup>* mice

A fragment of the murine *Casp1* gene was amplified by PCR from BAC clone RP23-424D5 (Source Bioscience) originating from a C57BL/6 mouse and used as a short arm (SA) for homologous recombination. The GCATGCCGT to GCAGCGCGT mutation at codon 284 was introduced into the long arm (LA) cloned from the same BAC template. Both fragments were cloned into the targeting vector pSPUC-DTA (Gewies et al., 2014). Sequence integrity was controlled by sequencing at GATC Biotech AG, Germany. *NotI*-linearized targeting vector was electroporated into R1/E (129S1/X1) or C57BL/6N embryonic stem cells. G418-resistant embryonic stem cells were screened by PCR combined with *HhaI* digest and Southern blot analysis. Clones that showed correct genomic integration of the targeting vector and presence of the *Casp1<sup>mit</sup>* mutation were injected into C57BL/6 blastocysts, which yielded chimeric males that displayed germline transmission of the *Casp1<sup>mit</sup>* allele. The floxed neomycin resistance cassette between exons 5 and 6 was removed by breeding to DEL-Cre mice (B6.C-Tg(CMV-cre)<sup>1Cgn</sup>/J), and the resulting mice were backcrossed 8 generations to the C57BL/6 background. Routine genotyping was performed by *HhaI* digest of PCR products amplified with the following primers: 5'- CCAAGGGAATTATTGCTGTCTTG-3' and 5'- GTGATATTCTGTGGTGACTAACCGA-3'.

### Generation of *Casp1<sup>-/-</sup>* in C57BL6 mice

Guide RNAs targeting exon 5 of the mouse *Casp1* gene were designed as described (Kayagaki et al., 2015) using the CRISPR Design website at <http://crispr.mit.edu> and ordered from Sigma Aldrich in RNA format using the gRNA sequence (including PAM) with the inverse sequence GAGGGCAAGACGTGTACGAGTGG (target ID: MM0000278298). Pronucleus injection of the gRNAs and Cas9 protein was done as described before (Hermann et al., 2014). The founders were screened by amplifying the region of interest by PCR with high-fidelity Phusion DNA Polymerase (ThermoFisher Scientific) and subsequent sequencing of the PCR product (GATC Biotech AG) using primers *Casp1\_E5 <sup>fwd</sup>*: TAGGAATTCGATGCTGAGAGCCTACCAGG and *Casp1\_E5 <sup>rev</sup>*: TCAGAATTCACCAGTACAGAACTAGCAAGGC, containing *EcoRI* restriction sites (underlined). Results were analyzed using CLC Main Workbench. Mice showing a heterogeneous DNA sequence in the region of interest were chosen for further analysis. To that end, the PCR product was cloned into the pCR2.1-TOPO TA vector (Thermo Fisher Scientific) and transformed into DH5α *E. coli* (NEB). DNA was isolated from seven different clones, sequenced, and analyzed for mutations causing a premature stop codon. The founder chosen for further breeding showed a TT insertion on one allele, leading to a translation stop in exon 5 of the *Casp1* gene. In addition, this mutation introduced a *BsrGI* restriction site (T∇GTACA). For genotyping the offspring, this restriction enzyme (NEB) was used on PCR products generated with the above-mentioned primers.

### Generation of *Gsdmd<sup>-/-</sup>* mice

Guide RNAs targeting exon 2 of the mouse *Gsdmd* gene were designed as described (Kayagaki et al., 2015) using gRNA sequence (including PAM) GGAGAAGGGAAAATTTCTGG. Injection of the gRNAs and Cas9 protein into C57BL/6 embryos was done as described before (Hermann et al., 2014). Biopsies for genotyping were taken at an age of 10-12 days. DNA extraction was performed using the KAPA HotStart Mouse Genotyping Kit according to the manufacturer's protocol. Genotyping PCR was done using Q5 Polymerase (NEB) using primers Oligo.507 (GSDMD\_ex2\_fw2; ggtgtgagccaccgtctat) and Oligo.508 (GSDMD\_ex\_rv2; ctgtggagggactccattgt), which were designed using Primer3 v.0.4.0 (<http://bioinfo.ut.ee/primer3-0.4.0/primer3/>), resulting in a fragment of 768 bp. The PCR product was sequenced using Oligo.507. This led to a 2 bp deletion in exon 2 of *Gsdmd* resulting in a premature stop codon.

### BMDC preparation and stimulation

Bone marrow-derived dendritic cells (BMDCs) were prepared from the tibiae and femora of 6-30 weeks old mice as previously reported (Groß et al., 2016; Schneider et al., 2013). Cells were grown in a humidified incubator at 37°C / 5% CO<sub>2</sub> in the presence of recombinant murine GM-CSF (20 ng/ml, Immunotools). After 6-9 days of differentiation, cells were harvested using 5 mM EDTA in 1x HBSS buffer and plated in 96-well plates at a density of 0.12-0.2 x10<sup>6</sup> cells per well in medium containing growth factor.

For stimulation of TLRs, cells were treated for 6h with the following concentrations of agonists: 20 ng/ml LPS, 10 µg/ml CpG DNA, 1 µg/ml R848, 0.1 µg/ml Pam<sub>3</sub>CSK<sub>4</sub>, 0.1 mg/ml Zymosan, 0.1 mg/ml Curdlan

(Wako). For inflammasome activation, cells were primed with 50 ng/ml *E.coli* K12 ultra-pure LPS for 3 hours and subsequently stimulated with inflammasome activators for 0.5-24h. Typical concentrations and incubation times if not indicated otherwise were as follows: 5  $\mu$ M nigericin (10  $\mu$ M for microscopy) for 45-60 min, 1  $\mu$ g/ml poly(dA:dT) for 3h (transfected with Lipofectamine 2000), 70  $\mu$ M Imiquimod for 2-3h, and MOI 20 *S. typhimurium* for 1-2h. For stimulation using bacteria, sterile LB-medium without antibiotics was inoculated with *Salmonella enterica* subspecies I serovar Typhimurium X3625 ( $\Delta$ aroA) (*S. typhimurium*) from a glycerol stock. After 12h at 37°C and 250 rpm, bacteria were subcultured in LB-medium diluted 1:20, 1:40, and 1:80 for another 3h at the same conditions. Samples with exponential growth rates (leading to Nlrp4-dependent, caspase-11 / Nlrp3-independent inflammasome activation, as previously described (Broz *et al.*, 2012)) were selected by measuring OD<sub>600</sub> using a BioPhotometer plus. Bacterial numbers were estimated by assuming OD<sub>600</sub> = 0.1 =  $1 \times 10^8$  colony-forming-units (cfu) per ml.

The caspase inhibitors Ac-YVAD-cmk (Enzo), Z-VAD-fmk (Enzo), Z-IETD-fmk (BioTechne), and VX-765 (a gift from Boehringer Ingelheim) were added to the cells at a concentration of 0.03-100  $\mu$ M as indicated after 2.5h of priming and 30 min prior to inflammasome activation. All inflammasome activators were carefully titrated and used at the lowest dose and the shortest time required to cause significant IL-1 secretion. All stimulations were performed in triplicates.

### Analysis of BMDC stimulations

Cytokines were quantified from cell-free supernatants by ELISA for murine IL-1 $\alpha$ , IL-1 $\beta$ , pro-IL-1 $\beta$  and TNF according to manufacturer's instructions (eBioscience). The IL-1 $\beta$  ELISA used is selective for the mature form of mouse IL-1 $\beta$ , while the pro-IL-1 $\beta$  ELISA only detects the pro-form since one of the antibodies is directed against the pro-domain (Dick *et al.*, 2016; Groß *et al.*, 2012; Schneider *et al.*, 2013). Cells were stimulated and measured in triplicates and values are shown as mean  $\pm$  s.e.m. (technical triplicates). For immunoblot analysis, triplicates of cell-free supernatants were pooled and combined with 3x SDS- and DTT-containing sample buffer (Schneider *et al.*, 2013). Cell lysates were prepared by washing cells with PBS and lysing them in the well in 1x sample buffer and pooling the triplicates. Supernatants and lysates were subjected to SDS-PAGE and transferred to nitrocellulose using standard techniques (Schneider *et al.*, 2013). To analyze inflammasome formation, the insoluble fraction of NP-40-lysed cells was subjected to immunoblot analysis, as previously described (Fernandes-Alnemri *et al.*, 2007). For immunoblotting of GSDMD, cytoplasmic fractions were prepared from BMDCs.  $2 \times 10^6$  cells were lysed in 100  $\mu$ l NP-40-containing lysis buffer and lysates were depleted of membranes by centrifugation to obtain cytoplasmic fractions.

Primary antibodies were as follows: goat anti-mouse IL-1 $\beta$  (AF-401, R&D Systems), mouse anti-mouse caspase-1 p20 (Casper-1, AdipoGen Life Sciences), mouse anti-mouse caspase-1 (Casper-2, AdipoGen Life Sciences), rabbit anti-ASC (AL177, AdipoGen Life Sciences), rat anti-mouse caspase-8 (1G12, Enzo), rabbit anti-mouse caspase-3 (#9661 and #9662, Cell Signaling), rabbit anti-GSDMD (G7422, Sigma), mouse anti- $\alpha$ -tubulin (B512, Sigma), rabbit anti-Vimentin (D21H3, Cell Signaling).

Cell death was determined by measuring LDH using the Promega CytoTox 96 Non-Radioactive Cytotoxicity kit according to the protocol. Medium served as blank value and was subtracted from the sample values. Results were plotted as percentage of 100 % dead cells lysed by repeated freeze-thaw cycles.

Caspase activity was analyzed by using the Promega CaspaseGlo® 1 Inflammasome assay according to the manufacturer's specifications. Cells were plated in white-walled 96-well plates and stimulated with nigericin for the indicated times. Medium without cells served as blank value and was subtracted from sample values. Luminescence was measured using a Mithras multimode microplate reader (Berthold).

For viability time course experiments, BMDCs were plated in 96 well cell culture plates ( $1 \times 10^5$  cells/well), cultured overnight at 37°C, primed with 50 ng/ml LPS for at least 3h and stimulated with nigericin (5  $\mu$ M) for various time-points up to 240 min. Cells were simultaneously harvested from plates by washing with 1x DPBS with 5 mM EDTA and stained with Annexin-V Pacific Blue 7-AAD Apoptosis Detection Kit (Biolegend). Samples were measured on a FACS Canto II (BD) and analyzed using FlowJo (FlowJo, LLC).

For membrane integrity experiments, BMDCs were seeded at  $3 \times 10^5$  cells/well in 8-well chambered coverslips (Ibidi), cultured overnight at 37°C, and primed with 50 ng/ml LPS for at least 3h. Nigericin (5  $\mu$ M), raptinal (10  $\mu$ M), or doxorubicin (10  $\mu$ M) were prepared in FCS supplemented phenol-red free FluoroBrite DMEM medium containing DRAQ7 (3  $\mu$ M). Following stimulation, cellular morphology (by DIC) and membrane integrity (by fluorescence imaging) were continuously observed for a time course of up to 16h by confocal microscopy on a Leica TCS SP8 confocal LSM equipped with a 63 $\times$  oil objective (NA 1.4, Leica Microsystems). The staining of the DNA by DRAQ7 indicated plasma membrane leakage.

## Immunophenotyping

Four 8 weeks-old *Casp1*<sup>+/+</sup> and B6.129-*Casp1*<sup>mit/mit</sup> mice each were sacrificed and spleens and cervical, axillary, and inguinal lymph nodes were harvested. Mice and organs were weighed, organs meshed, and red blood cell lysis was performed using G-DEX™ II RBC Lysis Buffer. Cells were counted using a hemocytometer and  $1.5 \times 10^6$  cells per organ were antibody-stained on a 96-V-bottom plate. First, cells were resuspended in live/dead stain eFluor 506 (1:1000 in 1x DPBS) and incubated for 10 min at 4°C in the dark. After that cells were washed and incubated in antibody mixtures for 30 min at 4°C in the dark. Cells were washed two times before immediate acquisition. All antibodies were diluted 1:400 in 1x DPBS + 2 % FCS except for anti-CD16/CD32, which was used at 1:200. Samples were analyzed by a FACS Canto II (BD Biosciences), data acquired by the DIVA software (BD Biosciences), and evaluated using FlowJo software (FlowJo, LLC). Compensation was performed using cells labeled with the corresponding antibodies for all conjugates according to the manufacturer's protocol. All antibodies were from eBioscience [eB] and Biolegend [BL]. Antibodies used were as follows: rat anti-mouse CD11c APC-conjugated (N418) [eB], rat anti-mouse CD16/CD23 (clone 93) [eB], rat anti-mouse CD19 eFluor 450-conjugated (1D3) [eB], rat anti-mouse CD21 FITC-conjugated (4E3) [eB], rat anti-mouse CD4 eFluor 450-conjugated (RM4-5) [eB], rat anti-mouse CD8 APC-conjugated (53-6.7) [eB], rat anti-mouse IgD APC-conjugated (11-26c) [eB], rat anti-mouse IgM PE-Cy5-conjugated (II/41) [eB], rat anti-mouse Ly6C PerCP-Cy5.5-conjugated (HK1.4) [BL], rat anti-mouse Ly6G PE-conjugated (1A8) [BL], rat anti-mouse CD11b PE-Cy7-conjugated (M1/70) [BL], rat anti-mouse CD11c APC-conjugated (N418) [BL], rat anti-mouse CD62L PerCP-Cy5.5-conjugated (MEL-14) [eB], rat anti-mouse CD44 APC-Cy7-conjugated (IM7) [eB], rat anti-mouse CD3 FITC-conjugated (17A2) [eB], rat anti-mouse B220 FITC-conjugated (RA3-6B2) [eB], rat anti-mouse B220 APC-Cy7-conjugated (RA3-6B2) [eB], rat anti-mouse I-A/I-E APC-Cy7-conjugated (M5/114.15.2) [BL].

## Immunofluorescence Imaging

For confocal immunofluorescence imaging of the ASC inflammasome, murine BMDCs were seeded at  $2 \times 10^5$  cells/well in 12-well culture slides (Ibidi). Cells were primed with 50 ng/ml of LPS for 2h and then stimulated with nigericin (10  $\mu$ M for 45 min) or left unstimulated. After treatment, the cells were washed with 1x DPBS, fixed in 4% paraformaldehyde for 10 min, and extracted in 1x DPBS with 0.1% (v/v) Triton-X100 for 5 min. Non-specific interactions were minimized by blocking with buffer containing 5% FCS and 0.1% Triton X-100 in 1x DPBS. Cells were stained overnight at 4°C with mouse anti-mouse caspase-1 (p10) (Casper-2, AdipoGen Life Sciences), rabbit anti-ASC antibody (AL177, AdipoGen Life Sciences), and (where mentioned) rat anti-mouse caspase 8 (1G12, Enzo) or rat anti-FLIP (Dave-2, Adipogen Life Sciences) diluted in blocking buffer. The anti-mouse Alexa Fluor 488 and anti-rabbit Alexa Fluor 555 were applied as secondary antibodies for double labelling while anti-mouse Alexa Fluor 488, anti-rat Alexa Fluor 555, and anti-rabbit Alexa Fluor 647 were used for triple staining at ambient temperature. All secondary antibodies were from Thermo Fisher Scientific. The slides were mounted in Prolong Diamond containing DAPI (Thermo Fisher Scientific). Confocal microscopy of immunostained cells was performed on a Leica TCS SP8 confocal LSM equipped with a 63x oil objective (NA 1.4) oil objective (Leica Microsystems) keeping the laser settings for imaging constant between samples for comparison. The images were acquired as z-stacks and compiled as maximum projection in 2D for display using the LAS X software package (Leica, Germany).

For improved optical resolution ( $\approx$  100 nm), the double labelled samples were also observed with an ELYRA PS.1 (Carl Zeiss Microimaging) microscope for structured illumination microscopy (SIM). Caspase-1 (p10) was labelled with anti-mouse Alexa Fluor 488 and ASC with anti-rat Alexa Fluor 555. Thin z-sections of ASC specks were collected in five rotations for each channel. Images were reconstructed using ZEN software (Carl Zeiss MicroImaging).

For higher optical resolution (<100 nm), stimulated emission depletion (STED) imaging was performed to better visualize the arrangement of caspase-1 and ASC in the ASC speck. Murine BMDCs were treated, fixed, extracted, blocked, and stained with primary antibodies towards caspase-1 (p10) and ASC as detailed above. The anti-mouse Alexa Fluor 594 and anti-rabbit Alexa Fluor 635 were applied as secondary antibodies (1:100 dilution) and 3D STED imaging was performed using a Leica SP8 STED 3X (Leica, Germany) equipped with a 100x oil objective (NA 1.4). A tunable white light laser source was used to optimally excite the applied fluorophores while depletion was performed at 775 nm for both Alexa Fluor 594 and Alexa Fluor 633. Images were collected in a sequential scanning mode using hybrid diode detectors to maximize signal collection while reducing background noise and the cross-talk between the channels. Image reconstructions were performed using the LAS X software package (Leica, Germany) and deconvolution was applied with the Huygens

Professional software package (Scientific Volume, the Netherlands). Line intensity profiles were also generated in LAS X software by drawing a line passing across the ASC speck.

### Mass Spectrometry Analysis

BMDCs from B6.129-*Casp1<sup>mit/mit</sup>*, -*Casp1<sup>-/-</sup>* and *Nlrp3<sup>-/-</sup>* mice were plated at  $1.5 \times 10^7$  cells per 100 mm plate and primed with 20 ng/ml LPS for 3h. Afterwards, four plates per genotype were treated with 5  $\mu$ M nigericin for 40 min and one plate each was left untreated. Replicates were kept individually at all times. Cell lysates, soluble and insoluble fractions of NP-40-lysed cells were prepared in SDS- and DTT-containing sample buffer as described above and subjected to SDS-PAGE. Proteins in the gel were visualized by Coomassie staining according to standard procedures and the protein amount per sample was estimated from comparison to a BSA-standard loaded onto the same gel. An equivalent of 8  $\mu$ g protein were subjected to alkylation with 55 mM chloroacetamide for 30 minutes and immediately afterwards, SDS-PAGE was performed. NuPAGE 4-20% Bis-Tris gels and NuPAGE MES SDS Running Buffer (both from Invitrogen) were used and electrophoresis was stopped as soon as the samples had entered the separating gel. Coomassie staining was done and the gel stored in 1 % acetic acid at 4°C until mass spectrometry analysis.

LC-MS/MS measurements were performed on an Eksigent nanoLC-Ultra 1D+ system (Eksigent, Dublin, CA) coupled to an Orbitrap Velos mass spectrometer (Thermo Fisher Scientific, Bremen, Germany). The dried samples were reconstituted in 20  $\mu$ L 0.1% FA, one half was loaded onto a trap column (100  $\mu$ m x 2 cm, packed in-house with 5  $\mu$ m C18 resin, Reprosil-PUR AQ material, Dr. Maisch) and washed using 0.1% FA for 10 min at a flow rate of 5  $\mu$ L/min. Accordingly, peptides were transferred to an analytical column (75  $\mu$ m x 40 cm, packed in-house with 3  $\mu$ m C18 resin, Reprosil-Gold C18 material, Dr. Maisch). During separation using a 225 min gradient from 4% to 32% solvent B (0.1% FA, 5% DMSO in 100% ACN) in solvent A (0.1% FA, 5% DMSO in HPLC-grade water) (Hahne *et al.*, 2013) at 300 nl/min flow rate, samples were directly injected into the Velos via ESI in positive ionization mode. The Velos was operated in DDA mode, automatically switching between MS1 and MS2 spectra both acquired in the Orbitrap mass analyzer. Full scan MS1 spectra (m/z 360 to 1300) were generated at a resolution of 30 000 using an automatic gain control (AGC) target value of 1e6 charges with a maximum injection time of 200 ms. Internal calibration was performed using a dimethyl sulfoxide cluster (m/z 401.922720). The top 10 peptide precursor peaks (isolation window 2 Th) were fragmented via HCD in the collision cell (normalized collision energy of 30%) using an AGC target value of 3e4 with a maximum injection time of 200 ms. Fragment ions (fixed first mass of 100 m/z) were recorded at a resolution of 7500 and dynamic exclusion was set to 20 s. Data analysis was performed using MaxQuant (version 1.5.1.0) (Cox and Mann, 2008) with the integrated search engine Andromeda (Cox *et al.*, 2011). For peptide and protein identification, raw files were searched against the UniProt mouse (010090) reference database (version 06/06/2014) annotated with Pfam. Carbamidomethylated cysteine was selected as fixed modification and oxidation of methionine as well as N-terminal protein acetylation as variable modification. Trypsin/P was selected as the proteolytic enzyme, with up to two missed cleavage sites allowed. Precursor tolerance was set to 6 ppm, and fragment ion tolerance, to 20 ppm. Peptide identifications required a minimal length of seven amino acids, and all data sets were adjusted to 1% PSM and 1% protein FDR. Feature matching between raw files was enabled, using a match time window of 2 min. Common contaminants and reverse identifications were filtered out. LFQ intensities calculated when a minimum of 2 peptides were quantified were used for the analysis (Cox *et al.*, 2014).

Mean values of quadruplicate LFQ values were calculated and the enrichment of proteins in samples from *Casp1<sup>mit/mit</sup>* mice over samples from *Casp1<sup>-/-</sup>* or *Nlrp3<sup>-/-</sup>* mice evaluated. Invers relative standard deviation (mean / SD) of *Casp1<sup>mit/mit</sup>* samples was used as an indicator for the specificity of detected proteins.

## SUPPLEMENTAL REFERENCES

Broz, P., Ruby, T., Belhocine, K., Bouley, D.M., Kayagaki, N., Dixit, V.M., and Monack, D.M. (2012). Caspase-11 increases susceptibility to *Salmonella* infection in the absence of caspase-1. *Nature* *490*, 288–291.

Cox, J., and Mann, M. (2008). MaxQuant enables high peptide identification rates, individualized p.p.b.-range mass accuracies and proteome-wide protein quantification. *Nature Biotechnology* *26*, 1367–1372.

Cox, J., Hein, M.Y., Lubner, C.A., Paron, I., Nagaraj, N., and Mann, M. (2014). Accurate proteome-wide label-free quantification by delayed normalization and maximal peptide ratio extraction, termed MaxLFQ. *Mol. Cell Proteomics* *13*, 2513–2526.

Cox, J., Neuhauser, N., Michalski, A., Scheltema, R.A., Olsen, J.V., and Mann, M. (2011). Andromeda: a peptide search engine integrated into the MaxQuant environment. *J. Proteome Res.* *10*, 1794–1805.

Dick, M.S., Sborgi, L., Rühl, S., Hiller, S., and Broz, P. (2016). ASC filament formation serves as a signal amplification mechanism for inflammasomes. *Nature Communications* *7*, 11929.

Fernandes-Alnemri, T., Wu, J., Yu, J.-W., Datta, P., Miller, B., Jankowski, W., Rosenberg, S., Zhang, J., and Alnemri, E.S. (2007). The pyroptosome: a supramolecular assembly of ASC dimers mediating inflammatory cell death via caspase-1 activation. *Cell Death Differ* *14*, 1590–1604.

Gewies, A., Gorka, O., Bergmann, H., Pechloff, K., Petermann, F., Jeltsch, K.M., Rudelius, M., Kriegsmann, M., Weichert, W., Horsch, M., et al. (2014). Uncoupling Malt1 Threshold Function from Paracaspase Activity Results in Destructive Autoimmune Inflammation. *CellReports* *9*, 1292–1305.

Groß, C.J., Mishra, R., Schneider, K.S., Médard, G., Wettmarshausen, J., Dittlein, D.C., Shi, H., Gorka, O., Koenig, P.-A., Fromm, S., et al. (2016). K<sup>+</sup> Efflux-Independent NLRP3 Inflammasome Activation by Small Molecules Targeting Mitochondria. *Immunity* *1–31*.

Groß, O., Yazdi, A.S., Thomas, C.J., Masin, M., Heinz, L.X., Guarda, G., Quadroni, M., Drexler, S.K., and Tschopp, J. (2012). Inflammasome activators induce interleukin-1 $\alpha$  secretion via distinct pathways with differential requirement for the protease function of caspase-1. *Immunity* *36*, 388–400.

Hahne, H., Pachi, F., Ruprecht, B., Maier, S.K., Klaeger, S., Helm, D., Médard, G., Wilm, M., Lemeer, S., and Kuster, B. (2013). DMSO enhances electrospray response, boosting sensitivity of proteomic experiments. *Nature Methods* *10*, 989–991.

Hermann, M., Cermak, T., Voytas, D.F., and Pelczar, P. (2014). Mouse genome engineering using designer nucleases. *J Vis Exp*.

Kayagaki, N., Stowe, I.B., Lee, B.L., O'Rourke, K., Anderson, K., Warming, S., Cuellar, T., Haley, B., Roose-Girma, M., Phung, Q.T., et al. (2015). Caspase-11 cleaves gasdermin D for non-canonical inflammasome signaling. *Nature* *1–18*.

Schneider, K.S., Thomas, C.J., and Groß, O. (2013). Inflammasome Activation and Inhibition in Primary Murine Bone Marrow-Derived Cells, and Assays for IL-1 $\alpha$ , IL-1 $\beta$ , and Caspase-1. In *Methods in Molecular Biology*, (Totowa, NJ: Humana Press), pp. 117–135.